Project: FP7-258033 MODE-GAP

Multi-mode capacity enhancement with PBG fibre

Project start date: 1st October 2010
Project completion date: 30th September 2014

Deliverable P10

Signal processing for optical MIMO transmission systems

July 2013

Dissemination Level		
PU	Public	**X**
PP	Restricted to other programme participants (including the Commission Services)	
RE	Restricted to a group specified by the consortium (including the Commission Services)	
CO	Confidential, only for members of the consortium (including the Commission Services)	

Table of Contents

Abstract 3

1. Introduction 3

2. Digital signal processing for the Transmitter 3

3. Transmission medium 4

3.1 Optical components 4

3.2 Transmission medium from a signal processing point of view 5

4. Digital signal processing for the Receiver 6

4.1 Optical front-end compensation 6

4.2 Chromatic dispersion compensation 7

4.3 MIMO equalization 7

4.4 Carrier phase estimation 8

5. Conclusions 8

6. References 8

Abstract

Adaptive multiple-input multiple-output (MIMO) digital signal processing is key to the current exploitation of spatial division multiplexing in high capacity optical transmission systems. This paper focuses on building blocks for the transmitter and receiver digital signal processing algorithms focusing on few-mode fiber systems. In addition, the estimation of the optical channel allows linear impairments to be mitigated hence the required optical performance monitoring algorithms are described.

1. Introduction

Recently, coherent signal transmission enabled by digital signal processing (DSP) has become the dominant solution for high capacity long haul transmission systems. Already well-established in the field of wireless communications, coherent transmission enables higher order quadrature amplitude modulation (QAM) constellations to be transmitted exploiting the in-phase and quadrature-phase components to increase the spectral efficiency. However, the usage of these constellations is limited by the optical signal to noise ratio (OSNR) requirements.

Even though optical time division and wavelength division multiplexing techniques can be exploited, the demand for even higher capacity continuously increases. However, as the single mode fiber capacity is currently nearing its theoretical capacity limits, causing a capacity crunch, other methods to further provide the required transmission system's capacity are necessary.

These key methods include limiting the transmitted channel's bandwidth by performing spectral shaping and pre-emphasis at the transmitter side enabling wavelength division multiplexed channels to be more closely spaced. However, the capacity gain is only approximately 2-fold, and hence limited in alleviating the impending capacity crunch. The other key method, which can potentially increase the transmission capacity is spatial division multiplexing (SDM).

This is achieved through three main contenders; the propagation of spatial modes along the same fiber core [1,2], by transmitting over individual cores of a multi-core fiber [3], or using a combination of the former two [4]. All provide a higher theoretical capacity than the currently employed single-mode fibers. MODE-GAP focuses on data transmission using increased core sizes, because of its beneficial nonlinear tolerances [5].

A transmission system consists of three key components: the transmitter (Tx), the transmission medium, and the receiver (Rx). First we briefly describe signal processing at the transmitter in section 2. Section 3 focuses on the few-mode optical domain and the corresponding optical performance monitoring in the digital domain through channel state information estimation providing key insights into the optical domain. The majority of the DSP is performed at the receiver side. The receiver DSP is detailed in section 4.

2. Digital signal processing for the Transmitter

In the transmitter, the DSP is limited to the main task of optimization of the transmitted data. Binary data sequences are concatenated with error correcting overhead [6]. Then, multiple binary sequences are combined to form constellations (symbols). To achieve the highest OSNR tolerance for each constellation, gray coding is applied before transmitting symbols [7]. For coherent transmission, the current standard is to use quadrature phase shift keying (QPSK). However, higher order constellations are becoming more prominent [1,8]. The biggest downside for higher order constellations is that the capacity scales logarithmically and OSNR tolerances becomes more stringent [9].

Further OSNR tolerance gain can be achieved by pre-emphasis on the symbols due to the use of independent digital-to-analog converters (DACs) to drive the individual arms of the IQ Mach Zehnder modulator, the transfer function of each arm can be pre-compensated. Fig 1a shows the required frequency spectrum without pre-emphasis. First the spectrum is bandwidth limited by applying a root raised cosine filter, the frequency spectrum output is depicted in fig 1b. This shapes the spectrum to a Nyquist bandwidth of $f_s = 1/T_s$, where f_s is the symbol rate, and T_s the symbol time. Next, a frequency gain filter is applied to compensate frequency dependent attenuation of the

electrical path and the optical modulator port. This is depicted in Fig 1c. The last filter performs the inversion of the modulator transfer function to linearize the total transmitter's transfer function. This especially becomes more important for higher order constellations.

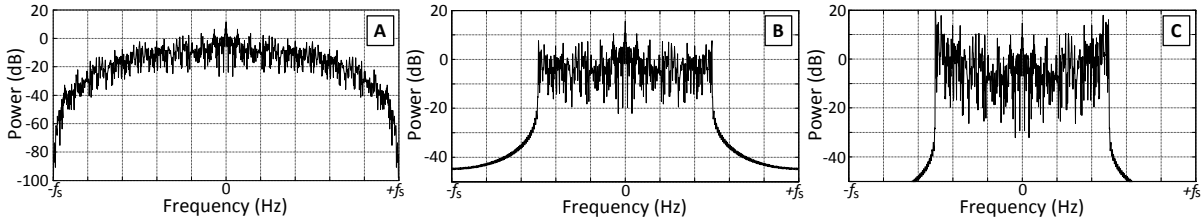

Fig 1. Frequency Spectrum at the transmitter side after A) constellation generation, B) root raised cosine filtering, and C) spectral pre-emphasis.

3. Transmission medium

The typical few-mode transmission medium consists of four key components, namely the mode multiplexer, the few-mode fiber, the few-mode erbium doped fiber amplifier (FM-EDFA), and the mode demultiplexer. In section 3.1 we describe the effects these components have on the transmission. In section 3.2 we show that performance monitoring can analyse these components in the digital domain.

3.1 Optical components

As spatial division multiplexing gains a growing interest, the current main focus is on few-mode fiber (FMF) transmission. According to the weakly guiding theory, modes propagating in optical fibers can be seen as linearly polarized (LP) modes [8]. Fig 2 depicts the mode profiles and their respective field distributions for the first two LP modes, the LP_{01} and LP_{11} modes [10]. Note that the second LP mode has two spatial degenerates. Effectively, three LP modes can be used as three orthogonal channels. Within each LP mode, two polarizations can be used. This results in 6 channels which can be simultaneously transmitted, as depicted in Fig. 2.

Each LP mode has its own propagation characteristics. The difference between the modal group velocities over a distance is the differential mode delay (DMD). However, not only the group velocity between LP modes differ, but also between polarizations, this is denoted as polarization mode delay (PMD). PMD occurs due to the slight elliptically of the optical fibers, creating a fast and slow axis. The strongest group velocity difference effect is DMD. These characteristics affect the impulse response of the system directly, and therefore the MIMO signal processing required in the receiver. By changing the refractive index profile of the fiber, the group velocity characteristics of the modes can be altered [11]. Each polarization within each LP mode also comes with its own attenuation and dispersion characteristics.

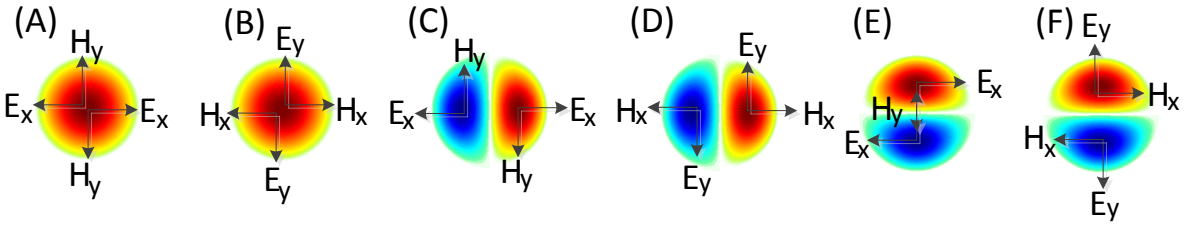

Fig 2. Mode field distributions for LP_{01} (A) X- and (B) Y-Pol, LP_{11a} (C) X- and (D) Y-Pol, and LP_{11b} (E) X- and (F) Y-Polarization.

To employ the modes as transmission channels, multiplexing components are required. At the transmitter and receiver a mode multiplexer (MUX) and demultiplexer (DMUX) is used, respectively. The first generation mode multiplexers and demultiplexers was based upon phase plates [12,13]. These allowed for separate excitation of modes. However, during transmission, the attenuation, signal amplification, and the coupling experienced by each

mode to each other causes an imbalance in the received power per transmitted channel, denoted as mode dependent loss (MDL). MDL causes a reduction in theoretical capacity [14]. Therefore, a second generation of mode multiplexers and demultiplexers have been developed within MODE-GAP based on the spot launching technique [15]. Each channel excites all modes equally, reducing the MDL. However more relevant to the potential for commercial implementation, integrated multiplexers [16], greatly reducing the size of the mode multiplexer and demultiplexer.

As optical fibers attenuate the transmitted signal, novel few-mode erbium doped fiber amplifiers (FM-EDFAs) are required [17]. Each LP mode is separately amplified by these FM-EDFAs. The difference in amplification per LP mode results in the differential mode dependent gain which effectively, is the same as mode dependent loss. In addition, optical FM-EDFAs are the only source in the transmission medium which add noise. This noise is additive white Gaussian noise (AWGN).

The combined components previously described are combined to form the transmission channel. This is depicted in Fig 3.

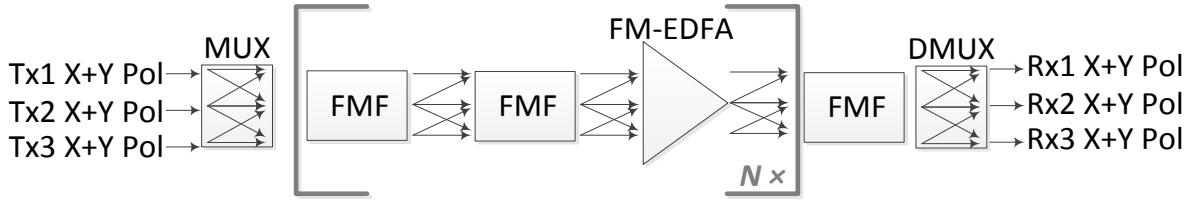

Fig 3. Optical transmission medium starts at the output of the 3 dual polarization transmitters, through the multiplexer, few-mode fibers and few-mode amplifier, and demultiplexer to the 3 dual polarization receivers.

3.2 Transmission medium from a signal processing point of view

The optical transmission system in section 3.1 can be described in the digital domain by the linear time invariant (LTI) equation $\widetilde{R} = HS + N$ at sample instance *k*, where $\widetilde{R}$ is the [6*K*×1] 2-fold oversampled received input vector, *H* the [6*K*×6] transmission matrix, *S* the [6×1] transmitted signal vector, *N* the [6*K*×1] additive white Gaussian noise (AWGN) vector. *K* denotes the number of impulse response samples per input, taps. Taps can be related to time, as $K = \frac{2\zeta}{T_s}$, where ζ is the total impulse response time of the system, and T_s is the symbol duration. However, in reality these systems are time variant and hence *H* has to be tracked over time. This can be described using the time variant description $H_{k+1} = H_k + P$, where *P* denotes the transition of *H* between sample *k* and *k*+1. To track this transition function, adaptive algorithms are required. This is further detailed in the receiver section.

The goal is to gain knowledge and estimate the transmission system and its respective characteristics. First it is important to establish K, the required impulse response length taken into account. In addition, the MDL characteristics need to be estimated. Knowledge of short term MDL allows for the outage probability to be estimated [18]. MDL estimation can be performed through the least-squares (LS) method, or the heuristic minimum mean square error (MMSE) method [19].

After transmission, the received and analog-to-digital converted input $\widetilde{R}$, can be defined as $\hat{R} = [r_1, r_2, \ldots r_6]$. The column-element *i* of *R* is defined as $r_i = \left[r_i(0), r_i(1), \ldots r_i\left(K+2L-1\right)\right]$, *L* is the number of training sequence symbols added as overhead. Let $R(f) = \mathcal{F}\{R\}$, where $\mathcal{F}\{\cdot\}$ denotes the element-wise Fourier transform. The transmitted sequence $S = [s_1^{\mathrm{T}}, s_2^{\mathrm{T}}, \ldots s_6^{\mathrm{T}}]$, where $^{\mathrm{T}}$ denotes the transpose. The column-element *i* of *S* is defined as $s_i = \left[s_i(0), 0, r_i(1), 0 \ldots r_i\left(L\text{-}1\right), 0\right]$. Note that s_i is 2-fold oversampled through zero-stuffing, and *L* is chosen to be 2^{13} bits. Let $S(f) = \mathcal{F}\{S\}^*$, where * is the complex conjugate.

Using the least-squares method, the transmission matrix *H* can be estimated as $H_{\mathrm{LS}} = \mathcal{F}^{-1}\{R(f) \otimes S^{\dagger}(f)\}$, where H_{LS} denotes the least-squares estimated transmission matrix, $\mathcal{F}^{-1}\{\cdot\}$ the element-wise inverse Fourier transform, $\otimes$ the Kronecker product, and † the pseudo-inverse. In reference to the MMSE section below, by using the zero-forcing method, the MIMO equalizer's weight matrix $W_{\mathrm{ZF}} = H_{\mathrm{LS}}^{\dagger}$. As can be seen from W_{ZF}, the zero-forcing method does not take noise into account.

The MMSE method, however, considers the impact of noise. The channel state information can be acquired either

by knowledge of the noise distribution, or by using a heuristic method. This heuristic method is readily present in optical MIMO systems, since an adaptive MIMO equalizer is used. This is further detailed in section 4. After the MIMO equalizer has converged, the inverse of the equalizer response is used to obtain the transmission matrix as $H_{\mathrm{MMSE}} = W_{\mathrm{MMSE}}^{\dagger}$. This inversion is similar to the zero-forcing method. By using MMSE CSI estimation, no additional computational overhead is required.

Finally, from the estimated transmission matrix H_{EST}, which is either H_{LS} or H_{MMSE}, the mode dependent loss can be determined. The singular value decomposition is used as $H_{\mathrm{EST}} = U\Lambda V^{\mathrm{H}}$, where U and V are unitary rotation matrices of sizes [6×6] and [6K×6K], respectively, and Λ is a [6×6K] rectangular diagonal matrix containing the real-valued non-negative eigenvalues λ_i of the transmission system. From the eigenvalues, the MDL in decibel is determined as $\mathrm{MDL} = 10{\cdot}\log_{10}(\max\{\lambda_1, \lambda_2, \ldots, \lambda_6\}^2/\min\{\lambda_1, \lambda_2, \ldots, \lambda_6\}^2)$. Note that instead of using H_{EST}, the respective weight matrices could also be used to determine the MDL.

4. Digital signal processing for the Receiver

The majority of the digital signal processing is performed at the receiver side, where transmission effects are compensated. For each transmitted mode, a coherent optical receiver is employed which consists of a hybrid mixer and a four balanced photodetectors to recover the I and Q components of the dual polarisation signals. After each optical receiver, the incoming signal is digitized by an analog-to-digital converter (ADC). In the digital domain, signal processing is performed. This is achieved using several stages, as depicted in Fig. 4. First, the optical receiver front end is compensated. Then, the accumulated chromatic dispersion (CD) is removed to shorten the fiber's impulse response, which allows for reduced the number K taps in the MIMO equalizer. This MIMO equalizer plays a key part in unraveling the mixed channels of the transmission system. Due to the nature of coherent transmission using a local oscillator, a frequency offset is inevitably present. This frequency offset is removed by carrier phase estimation (CPE). Finally, we perform timing recovery on each unraveled output separately. We address these key blocks in this section in detail.

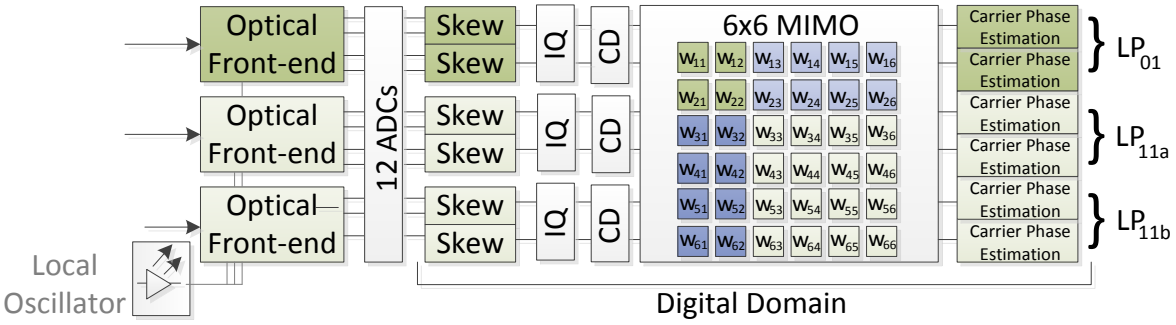

Fig. 4 Two mode (LP01 and LP11) MIMO receiver employing three dual polarization coherent optical receivers, 12 analog-to-digital converters, skew and IQ-Imbalance compensation algorithms, chromatic dispersion removal, a 6 × 6 MIMO equalizer, and carrier recovery.

4.1 Optical front-end compensation

Generally, transmission channels are described as complex filters where both quadratures of the signal have equal impairments. However in reality, both inphase and quadrature (IQ) components are processed separately. These components experience different attenuation and phase impairments, due to receiver imbalances. We refer to this as IQ-imbalance. These impairments are caused by incorrectly set IQ bias point at the transmitter, responsitivity differences of the photo detectors, electrical lines, and ADC imperfections. This leads to a DC-offset for each quadrature, and a general imbalance. In addition, timing mismatches can occur as well. These timing mismatches can easily be compensated by interpolation of the inputs. To compensate IQ imbalance, we can use Gram-Schmidt or Löwdin Orthogonalization [20].

4.2 Chromatic dispersion compensation

Dispersion compensation consists of two key stages, namely chromatic dispersion estimation, and chromatic dispersion compensation. One key benefit of SDM is that the transmitted channels become fully mixed, resulting in the same chromatic dispersion effects for each channel. Hence, chromatic dispersion can be seen as a common-mode impairment. At the receiver side, the chromatic dispersion of only a single channel is required to be estimated. This can then be applied to all transmitted channels. Alternatively, if the chromatic dispersion of the system is known, the chromatic dispersion can be compensated efficiently through a static frequency domain filter [20,21].

4.3 MIMO equalization

Adaptive equalization and tracking of H consists of two stages, namely linear filtering using a fractionally spaced adaptive weight matrix W, and an adaptive algorithm. To optimize the [6×1] system output $R = W\widetilde{R}$, the LMS algorithm heuristically minimizes the function $\left|W\widetilde{R} - S\right|$, where W is of the size [6×6K]. From this, it is clear that MMSE takes noise into account during the adaptive tracking of H. Therefore $W \neq H^{\dagger}$, but W is a close approximation of the pseudo inverse of the channel matrix H. By using the adaptive algorithm of the MIMO equalizer, the weight matrix W is updated. Note that W is updated depending on the output error. The output error at sample instance k is given by $e = d - R$, where e is the output error, a [6×1] vector, and d is the [6×1] vector of the desired signal. For the Least Mean Squares (LMS) algorithm this is the training symbol value, and for decision directed (DD) LMS this is the maximum likelihood symbol. At time instance k, W is updated using $W_{k+1} = W_k + \mu e\widetilde{R}^{\mathrm{H}}$, where μ is a constant step size, and $^{\mathrm{H}}$ denotes the Hermitian transpose.

The step size is an important value, as it determines both the final error, as well as the convergence time. Having a larger or smaller step size than is required causes additional bit errors, because of a noise floor caused by the step size, or improper channel tracking capabilities, respectively. Note that the convergence time is inversely proportional to the step size and gives insight to the system's adaptive tracking capabilities. For fast tracking, a high step size is desirable, however for a low final error value, a small step size is preferred. Also note that, for a stable system, the maximum step size has to be constrained.

The W matrix can be subdivided into 6 row vectors, denoted as W_i, of size [1×6K], where i denotes the respective output [22]. Only the terminology changes, while the complexity remains the same. However, as shown in the previous paragraphs, a weight matrix is adapted by the step size μ. By subdividing W, each weight matrix W_i can use its respective step size μ_i. Now that each output has its own step size, it is possible to adaptively change the step size on a per output basis, according to the needs whether it is tracking capabilities, or minimizing the output error, as depicted in Fig. 5. At time instance k, a lookup table is used to map the averaged output error $e_{av}[i]$ to a corresponding step size μ_i. By using the LUT, the system BER remains equal to the optimal fixed step size system. However, the convergence time can be greatly reduced [22]. In addition, optimizing the fixed step size is no longer necessary, as the adaptive step size optimizes between the best BER and tracking capabilities. However, this comes at the expense of added complexity in the MIMO equalizer.

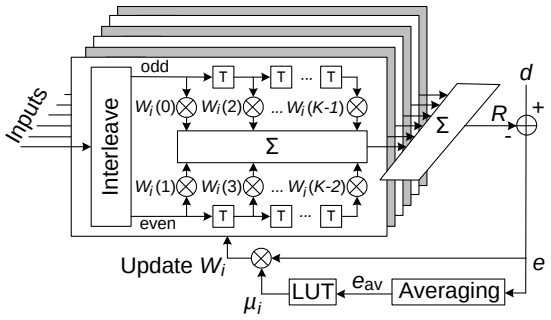

Fig. 5 Single output equalization using an adaptive step size determined by a lookup table.

4.4 Carrier phase estimation

After MIMO processing has been performed, the carrier offset is removed. In offline-processed optical transmission sytems, generally, this is either performed by the 4th order Viterbi-Viterbi algorithm, or by a phase detector (PD) and digital phase locker loop (DPLL) [23,24]. In our implementation, we have chosen for the latter.

Traditionally, each received channel requires one carrier recovery stage, as depicted by Fig. 6. Therefore, the complexity of the carrier recovery scales linearly with the number of transmitted channels. However, besides chromatic dispersion, carrier phase estimation is the second common-mode impairment due to the sharing of the local oscillator laser. Therefore it is possible to use either a master/slave setup [25], or the carrier information of multiple channels, as depicted in Fig. 6. The joint CPE algorithm takes the phase correlation of both polarizations into account and therefore uses only the information of one polarization, hence reducing the number of phase detectors by 50%. This has the most significant reduction in DSP complexity while the OSNR tolerance remains unimpaired. The only overhead required is 3 summations and 1 division.

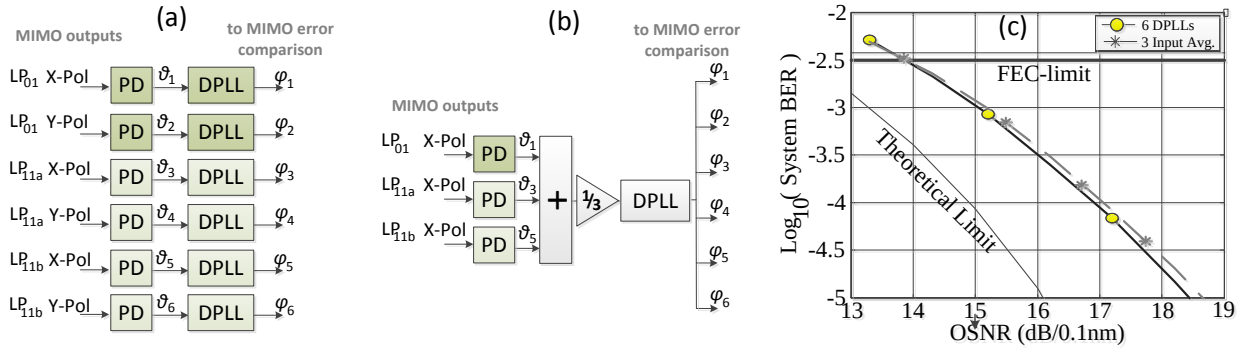

Fig. 6 (A) Traditional carrier phase estimation scheme. (B) Joint carrier phase estimation scheme. (C) Performance of traditional and proposed schemes for an 80 km transmission experiment [26].

5. Conclusions

This report provides a detailed description of the digital signal processing building blocks used in the MODE-GAP project, both at the transmitter and receiver side. The majority of the signal processing is performed at the receiver side. At the receiver side, the key building blocks are front-end compensation, (joint) chromatic dispersion compensation, multiple-input multiple-output equalization, and (joint) carrier phase estimation.

In addition, a separate building block has been described which allows for optical performance monitoring. This is used to investigate the performance of optical components.

6. References

[1] R.G.H. van Uden *et al.*, "Adaptive Step Size MIMO Equalization for Few-Mode Fiber Transmission Systems," *Proc. ECOC*, paper We.3.D.2 (2013).

[2] V.A.J.M. Sleiffer et al., "73.7 Tb/s (96x3x256-Gb/s) mode-division-multiplexed DP-16QAM transmission with inline MM-EDFA," *Proc. ECOC*, paper Th.3.C.4 (2012).

[3] H. Takara et al., "1.01-Pb/s (12 SDM/222 WDM/456 Gb/s) Crosstalk-managed Transmission with 91.4-b/s/Hz Aggregate Spectral Efficiency," *Proc. ECOC*, paper Th.3.C.1 (2012).

[4] C. Xia et al., "Hole-Assisted Few-Mode Multicore Fiber for High-Density Space-Division Multiplexing," *Photonics Technology Letters*, vol.24, no.21, pp.1914-1917 (2012).

[5] D. Rafique et al., "Impact of power allocation strategies in long-haul few-mode fiber transmission systems," Optics Express, Vol. 21, No. 9 (2013).

[6] F. Kschischang, "Introduction to Forward Error Correction," *tutorial at OFC*, SC 390 (2013).

[7] F. Gray, Pulse code communication, U.S. Patent 2,632,058 (1953).

[8] R. Ryf et al.,"32-bit/s/Hz Spectral Efficiency WDM Transmission over 177-km Few-Mode Fiber," *Proc. OFC*, paper PDP5A (2013).

[9] R.-J. Essiambre et al., "Capacity Limits of Optical Fiber Networks," Vol. 28, No. 4, pp. 662-701 (2010).
[10] D. Gloge, "Weakly Guiding Fibers," Appl. Opt. 10, 2252-2258 (1971).
[11] L. Grüner-Nielsen *et al.*, "Few Mode Transmission Fiber with low DGD, low Mode Coupling and low Loss," *Proc. OFC*, paper PDP5A (2012).
[12] R.G.H. van Uden et al., "Phase plate tolerances in a tri-mode demultiplexer," *Proc. IEEE Summer Topicals, pp. 216-217* (2012).
[13] V.A.J.M. Sleiffer et al., "Mode-division-multiplexed 3x112-Gb/s DP-QPSK transmission over 80-km few-mode fiber with inline MM-EDFA and Blind DSP," *Proc. ECOC*, paper Tu.1.C.2 (2012).
[14] P.J. Winzer and G.J. Foschini, "MIMO capacities and outage probabilities in spatially multiplexed optical transport systems," *Optics Express*, Vol. 19, No. 17 (2011).
[15] H Chen et al. "3 x MDM x 8 WDM x 320-Gb/s DP-32QAM Transmission over a 120km Few-Mode Fiber Span Employing 3-Spot Mode Couplers," *Proc. OECC*, paper PD3-6 (2013).
[16] H. Chen et al., "Demonstration of a photonic integrated mode coupler with 3.072Tb/s MDM and WDM transmission over few-mode fiber," *Proc. OECC*, PD2-5 (2013).
[17] Y. Jung et al., "Three mode Er3+ ring-doped fiber amplifier for mode-division multiplexed transmission," *Optics Express*, *21*(8), 10383-10392 (2013).
[18] S. Randel *et al.*, "Adaptive MIMO Signal Processing for Mode-division Multiplexing," *Proc. OFC* (2012).
[19] R.G.H. van Uden *et al*., "Performance Comparison of CSI Estimation Techniques for FMF Transmission Systems," *Proc. IEEE Summer Topicals*, paper WC 4.2 (2013).
[20] S.J. Savory, "Digital Coherent Optical Receivers: Algorithms and Subsystems," *IEEE Journal of Selected Topics in Quantum Electronics*, vol.16, no.5, pp.1164-1179 (2010).
[21] R.A. Soriano *et al.*, "Chromatic Dispersion Estimation in Digital Coherent Receivers," *Journal of Lightwave Technology*, vol.29, no.11, pp.1627-1637 (2011).
[22] R.G.H. van Uden *et al*., "Adaptive Step Size MIMO Equalization for Few-Mode Fiber Transmission Systems," *Proc. ECOC*, paper Th.2.C.2 (2013).
[23] X. Zhou et al., "An Improved Feed-Forward Carrier Recovery Algorithm for Coherent Receivers With M-QAM Modulation Format," *Photonics Technology Letters*, vol.22, no.14, pp.1957-1960 (2010).
[24] M. Taylor, "Phase Estimation Methods for Optical Coherent Detection Using Digital Signal Processing," *Journal of Lightwave Technology*, vol. 27, no. 7, pp. 901–914 (2009).
[25] R.G.H. van Uden *et al*., "Employing a single DPLL for joint carrier phase estimation in few-mode fiber transmission," *Proc. OFC*, paper OM2C.1, 2013.
[26] R.G.H. van Uden *et al*., "Single DPLL Joint Carrier Phase Compensation for Few-Mode Fiber Transmission," *Photonics Technology Letters*, *25*(14), 1381-1384 (2013).